Effects of coadsorbed atomic oxygen on the electron-stimulated desorption of neutral NO from Pt(111)

A. R. Burns, E. B. Stechel, D. R. Jennison, and T. M. Orlando
Sandia National Laboratories, Division 1151, Albuquerque, New Mexico 87185
(Received 21 June 1991; revised manuscript received 16 September 1991)

We examine the effects of an electronegative coadsorbate on the electron-stimulated-desorption (ESD) yield and desorbate energies (translational and internal) of a chemisorbed molecule. Specifically, we use laser resonance-ionization spectroscopy to characterize the ESD of neutral NO from a Pt(111) surface precovered with atomic oxygen. With increasing oxygen coverage (up to 0.75 monolayer), we observe the following for the NO desorbate: (1) an exponential increase in specific yield, (2) increased translational energy, (3) decreased vibrational energy, (4) decreased rotational energy, and (5) a growing propensity to produce the upper spin-orbit level of the spin-orbit-split electronic ground state. The first three observations are understood in terms of an O-induced reduction in charge transfer from the substrate into the adsorbate 2π molecular level to screen the electronic excitation ($5\sigma^{-1}$). This has the dual effect of reducing the Auger decay rate $5\sigma^1 2\pi^2(\mathrm{NO}) \rightarrow 5\sigma^2 2\pi^0(\mathrm{NO}^+)$, and of lowering the NO vibrational excitation. The consequences of a reduced Auger decay rate are a larger ESD yield and more desorbate translational energy. We argue that the spin-orbit propensity arises from an O-induced rotational hindering of the NO excited state. A hindered NO^+ rotor, ionized after Auger decay, is reneutralized by a strongly spin-orbit-split Pt(111) substrate at a greater rate into the upper level than into the lower level.

I. INTRODUCTION

Often referred to as "poisons" and "promoters" in the surface science community, electron-withdrawing (e.g., O and S poisons) and electron-donating (e.g., K promoters) coadsorbates can greatly modify the physical characteristics of adsorbed molecules[1] and thus influence the rates of surface chemistry. As revealed by thermal desorption and vibrational spectroscopy, coadsorption induces changes in adsorbate-surface and intramolecular bond strengths. These changes may derive from different adsorption geometries,[2,3] electrostatic interactions with the coadsorbate,[4] or a different charge state of the adsorbate.[5-7] Similarly, shifts in electronic binding energies of adsorbed molecules can be used to examine the effects of coadsorbates on charge-transfer screening of the adsorbate valence or core holes by the substrate.[1] Most importantly, it can be said in general terms that active coadsorbates alter the local electron density at the adsorption site.

Because stimulated surface processes such as electron- or photon-stimulated desorption (ESD) involve the rupture of surface and adsorbate bonds due to electronic excitation and subsequent atom motion in the excited state,[8,9] they can be extremely sensitive probes of changes in the local electronic environment. For example, the ESD yields of CO^+ and NO^+ from K-covered Ni(111) are reduced by a factor of 50 relative to the clean surface.[10] A significant drop in the photodesorption of NO from K-covered Si(111) has also been reported.[11] Conversely, ESD ion yields have been shown to increase in the presence of coadsorbed O.[10,12] The photodesorption yield of neutral NO from Ni(111) also increases in the presence of O.[13,14] In the present work we report a greater than 90-fold increase in the ESD yield of neutral NO from a Pt(111) surface when it is precovered by 0.75 monolayer (ML) of atomic oxygen. Our purpose here is to examine in complete detail how coadsorbates affect the highest-probability electronically stimulated processes, i.e., those which produce neutral desorbates. In particular, we discuss the effects of coadsorbed atomic O on the ESD of NO from Pt(111), which has been studied extensively in the absence of coadsorbates.[15-18]

For molecules chemisorbed on transition metals, some excited-state lifetimes are an intimate function of the virtually instantaneous electronic screening of the excitation by substrate charge transfer.[15,18-20] Since substrate screening generally reduces adsorbate electronic binding energies, ultraviolet (UPS) and x-ray photoelectron spectra have been used extensively to probe screening effects in the binding-energy shifts of molecular levels of chemisorbed NO and CO.[3,21-26] The presence of the electron-withdrawing O increases binding energies, therefore indicating a decrease in substrate screening of core and valence holes. We show here that a reduction in substrate screening by the presence of the oxygen can also increase lifetimes of excited states responsible for desorption.

Changes in charge-transfer screening not only affect electronic excitation lifetimes, but can also alter the degree of vibrational and rotational excitation of the desorbed molecules.[15,20] Internal excitation is particularly pronounced if substrate screening is through a strongly antibonding molecular orbital of the adsorbate, such as the 2π orbital of NO. Vibrational excitation of desorbed NO from the clean surface revealed the presence of charge-transfer substrate screening of the deep valence excitation through the 2π levels.[15,18,19] (By "clean" sur-

face, we refer to the absence of coadsorbates such as atomic O. There are, in fact, no other measurable impurities on the surface at any time.)

The NO+O/Pt(111) coadsorption system was chosen because it has been well characterized with UPS, vibrational high-resolution electron-energy-loss spectroscopy (HREELS), and thermal desorption by Bartram, Koel, and Carter.[3] Another important aspect in these studies is the absence of bond formation between NO and O, even at the highest oxygen coverages ($\Theta_O=0.75$ ML). The study of electropositive coadsorbates [e.g., NO+K/Pt(111)] is less favorable because there may exist direct electrostatic interactions between NO and K,[25] analogous to that observed for CO+K/Pt(111).[4] Finally, the ESD yield of NO *increases* with O coverage, making it amenable to state-selective, laser resonance-ionization detection methods[15,19,20] yielding quantum-specific information on the yield, threshold, translational and internal energies of NO ESD. We show that complete characterization reveals not only an enhanced yield relative to the clean surface, but also significant shifts in the translational energy, changes in the vibrational and rotational excitation, and a definite propensity for populating the $\Omega=\frac{3}{2}$ spin-orbit state for the open shell $^2\Pi_{\Omega=3/2,1/2}$ ground-state molecule.

It has been well established that NO adsorbs at *both* bridge and atop (terminal) sites on clean Pt(111).[3,27] However, at $\Theta_O>0.25$ ML precoverages, NO adsorbs *only* at atop sites.[3] Atomic oxygen occupies threefold hollow sites at $\Theta_O=0.25$ ML, in a $p(2\times2)$ ordered array.[28,29] As Θ_O increases, the hcp hollow sites become occupied and the ordering is slowly lost. At $\Theta_O=0.60$ ML, the $p(2\times2)$ structure is still visible, while it is faint at the maximum $\Theta_O=0.75$ ML.[28] There is no HREELS or UPS evidence of O_2 bond formation, nor is there any evidence for different site occupation at the highest coverages.[28]

II. EXPERIMENT

All experiments discussed below were conducted in an ion-pumped vacuum chamber with a base pressure below 5×10^{-11} Torr. The chamber is equipped with a cylindrical mirror analyzer for Auger electron spectroscopy (AES), a quadrupole mass spectrometer for thermal desorption spectrometry (TDS), a pulsed electron gun, and a multichannel plate time-of-flight (TOF) apparatus for the detection of ions produced by laser resonance-ionization of desorbed neutral desorbates. Details concerning the TOF geometry have been published elsewhere.[15,19,20] The polished Pt(111) crystal[30] was resistively heated to 1200 K and cooled to less than 90 K. A type-K (chromel-alumel) thermocouple contacts the side of the crystal for temperature measurements. The Pt crystal was initially cleaned by resistive heating and ion bombardment cycles, followed by annealing at 1200 K. Cleanliness was confirmed by the absence of C(*KLL*), Ca(*LMM*), O(*KLL*), etc., in the AES. After initial cleaning, the crystal was recleaned by resistive heating.

The Pt(111) surface was precovered with O atoms by heating it to 400 K while dosing with NO_2, which thermally dissociates. The NO product rapidly desorbs, leaving only the O atoms on the surface.[3,28] The NO_2 (99.995% purity) was handled in a passivated stainless-steel gas manifold equipped with a glass cold finger for freeze-pump-thaw degassing of impurities. The passivated dosing port consists of a small tube (effusive source) in front of the crystal which allows for high dose rates without letting the chamber pressure exceed 2×10^{-10} Torr. This was particularly important in order to reduce background NO due to NO_2 decomposition on the chamber walls. The maximum oxygen coverages obtained with this method were $\Theta_O=0.75$ ML, as verified by the 0.90 ratio of the AES peak heights $I(O(KLL,510\text{ eV}))/I(\text{Pt}(238\text{ eV}))$.[31] All Θ_O were measured with AES before dosing the sample with NO; the depletion of the O layer due to the Auger electron beam was negligible.[20,28]

The O-covered sample was kept at 200 K while dosing with NO so that only well-defined chemisorbed states (bridge and atop) of NO formed; i.e., uncharacterized states that give rise to low-temperature desorption peaks (<200 K) were absent.[3] In all experiments discussed here, saturation coverages of NO were used. Following dosing, the crystal was rotated away from the dosing port and allowed to rapidly cool to below 90 K, the temperature at which all data were collected. TDS of the sample following data acquisition revealed NO and O_2 peaks that were qualitatively similar to those observed previously for various values of Θ_O.[3,27] (A sample NO TDS run for $\Theta_O=0.75$ ML is shown at the top of Fig. 6.) A high-temperature tail ($T>425$ K) was observed for the NO peak, which can be attributed to desorption from crystal supports rather than from defects. This was confirmed by the lack of N_2 and O_2 desorption from the clean surface, which commonly follows NO dissociation at defect sites.[27]

Although extensive details concerning data-acquisition methods for laser resonance-ionization detection of ESD neutral desorbates have been published,[19,20] a few important features merit repeating. All the experiments were conducted in the TOF mode whereby the burst of neutral particles produced by a 0.3–1.2-μs electron-beam pulse (1.6×10^{16} electrons/cm^2 s during the pulse) traverse a 0.5-cm distance before being resonantly ionized at a specified delay time by a 4-ns laser pulse. A ribbon-shaped laser-beam area of ~0.5 cm^2 (0.1 cm thick) is sufficient to angle-integrate most of the neutral particles. The TOF translational energy (E_{trans}) distributions were obtained by computer-programmed steps in delay time (after a 300-ns electron pulse), corresponding to linear steps in desorbate translational energy.[20] Although the data were automatically scaled in energy and corrected for the velocity dependence of the particle density in the laser beam, there is still an intrinsic error due to the velocity spread ($\Delta V/V$) from the electron-beam pulse width, which increases with decreasing delay time. In order to properly correct for this, however, the actual velocity distribution must be known beforehand. Thus, for the present experiments, the TOF E_{trans} distributions are best suited for observing relative changes (e.g., due to changes in oxygen coverage), rather than for assigning

absolute energies.

Threshold measurements were obtained by simultaneously sweeping the electron-beam energy (E_{HV}) and focus for a fixed E_{trans} (i.e., delay time). The focus and energy of the electron beam were computer-controlled to insure a constant spot size (0.016 cm^2) on the sample (0.78 cm^2). At $E_{HV} < 20$ eV, however, it becomes difficult to keep the beam spot size from increasing beyond the sample diameter. To make sure that the threshold data referred only to NO on the Pt(111) crystal, it was necessary to subtract background signal from crystal mounts, etc. This was accomplished by thermally desorbing NO from the Pt substrate at 350–400 K, recooling the crystal, and repeating the scan.

The NO rotational spectrum for a given vibrational level v'' was obtained by scanning the laser through the $A\,^2\Sigma^+(v') \leftarrow X\,^2\Pi_{1/2,3/2}(v'')$ resonance-enhanced (1+1) ionization[32,33] for a fixed E_{HV} and E_{trans}. Saturation and alignment effects[33] for the mean 40-mJ/cm^2 laser intensity were calibrated by comparison of calculated rotational intensities[34] with the room-temperature $v=0$ NO gas-phase spectrum, acquired for NO bled into the vacuum chamber. All rotational spectra were collected with laser pulse energies within 15–20% of the mean energy as determine by a pyroelectric detector; data at laser energies falling outside this distribution were rejected.

III. RESULTS

A. NO translational energy distributions

The TOF E_{trans} distributions for desorbed NO were examined as a function of oxygen coverage and internal energy. The electron-beam energy was 350 eV (changes in E_{trans} with E_{HV} were not observed). Normalized E_{trans} distributions for NO ($v=0$) as a function of oxygen coverage (Θ_O) on the Pt(111) surface are shown in Fig. 1. Clearly, there is a pronounced shift in the distributions to higher energy with increasing oxygen coverage. The shift becomes evident at $\Theta_O > 0.4$ ML. The E_{trans} distribution at the highest Θ_O (0.75 ML) is characterized by a sharp

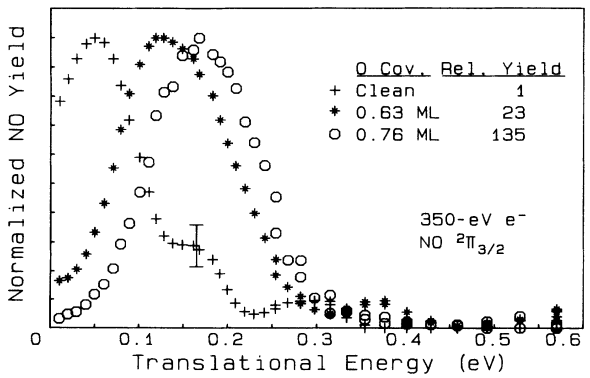

FIG. 1. Comparison of the normalized TOF E_{trans} distributions for the ESD of NO ($v=0$, $J=9.5-11.5$ P_{12} band head) as a function of O-atom coverage (Θ_O) on Pt(111).

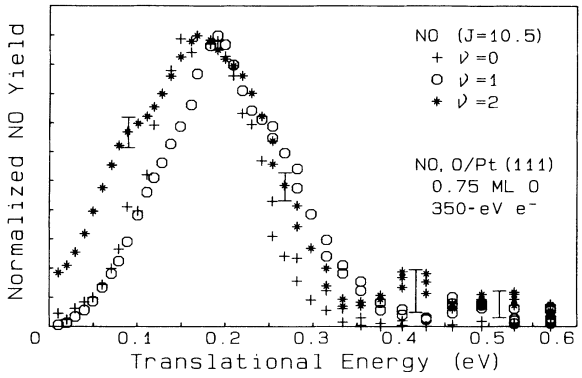

FIG. 2. Comparison of the TOF E_{trans} distributions for the three observed vibrational levels ($v=0,1,2$) for the ESD of NO on $\Theta_O=0.75$-ML precovered Pt(111). The data were acquired at the P_{12} band head ($J=9.5-11.5$) and normalized with respect to the peak (not to the actual yield) for the purpose of comparison.

peak centered at 0.18 eV and a low-energy tail which goes to zero at the lowest energies. This contrasts strongly with the E_{trans} distribution from the clean surface ($\Theta_O=0$ ML, $\Theta_{NO}\approx 0.5$ ML), which has significant yield only at the very lowest energies (0.05-eV peak) and has a low-energy cutoff.[15]

When the NO E_{trans} distribution for $\Theta_O=0.75$ ML is examined as a function of vibrational energy ($v=0,1,2$), one can see in Fig. 2 that there are no substantial differences in peak energies, although there is a broadening in the $v=2$ distribution at the lowest E_{trans} energies.

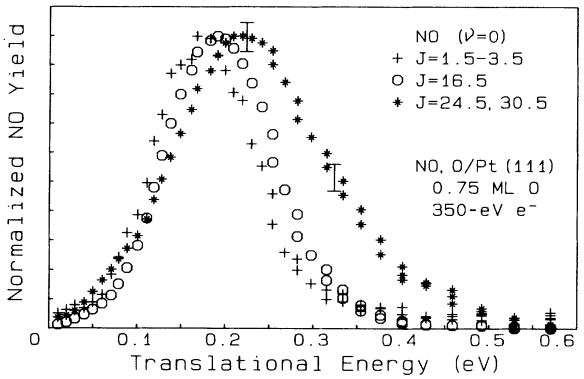

FIG. 3. Comparison of the TOF E_{trans} distributions as a function of rotational energy (E_{rot}) for the ESD of NO ($v=0$) on $\Theta_O=0.75$-ML precovered Pt(111). The low-J distribution was obtained at the $P_{22}Q_{12}$ band head ($J=1.5-3.5$, $E_{rot}=15$ cm^{-1}). The intermediate-J distribution was obtained at the $R_{12}Q_{22}$ ($J=16.5$, $E_{rot}=483$ cm^{-1}) line. The high-J distribution was obtained with the R_{22} ($J=24.5$, $E_{rot}=1045$ cm^{-1}) line which overlaps with the weaker (~ 2.2) $R_{12}Q_{22}$ ($J=30.5$, $E_{rot}=1606$ cm^{-1}) line. The TOF distribution for the $R_{12}Q_{22}$ ($J=21.5$, $E_{rot}=809$ cm^{-1}) line is not plotted because it is identical to the high-J distribution. All distributions were normalized with respect to the peak.

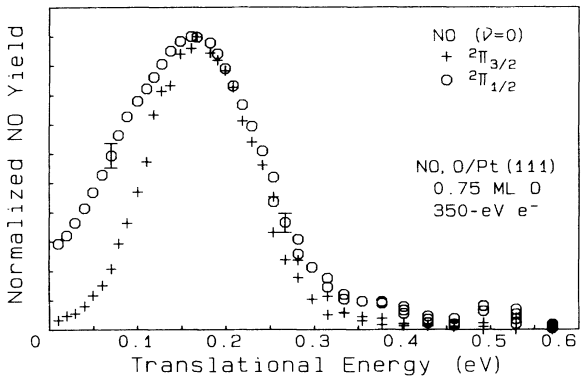

FIG. 4. Comparison of the TOF E_{trans} distributions for the $\Omega=\frac{3}{2},\frac{1}{2}$ spin-orbit levels for the ESD of NO ($v=0$) on $\Theta_O=0.75$-ML precovered Pt(111). The $\Omega=\frac{3}{2}$ data were acquired at the $^2\Pi_{3/2}P_{12}$ band head ($J\approx 9.5-11.5$), while the $\Omega=\frac{1}{2}$ data were acquired at the $^2\Pi_{1/2}P_{11}$ band head ($J\approx 8.5-10.5$).

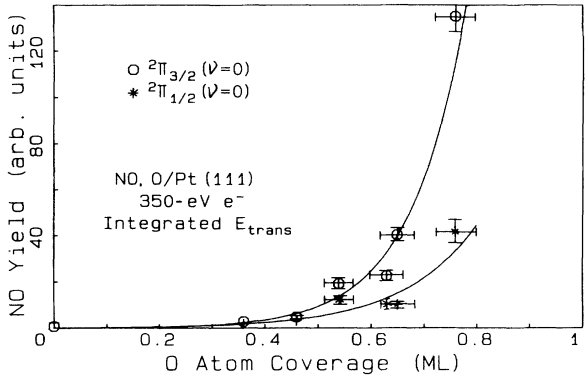

FIG. 5. Enhancement in the specific NO ($v=0$) ESD yield as a function of O-atom coverage (Θ_O). The specific NO yield for each spin-orbit state $^2\Pi_{1/2,3/2}$ was obtained at the P_{12} ($\Omega=\frac{3}{2}$, $J\approx 9.5-11.5$) and P_{11} ($\Omega=\frac{1}{2}$, $J\approx 8.5-10.5$) band heads. The solid curves are single exponential fits.

Higher vibrational populations ($>v=2$) were not detected. On the clean surface the higher vibration ($v=2,3$) E_{trans} distributions revealed an additional "high-" energy channel centered about 0.3 eV and extending beyond 0.6 eV. This high E_{trans} channel is either absent for the $v=2$ distribution at $\Theta_O=0.75$ ML or is obscured by the large yield of the dominant channel at 0.18 eV.

Rotationally resolved E_{trans} distributions for NO ($v=0$) ESD from the $\Theta_O=0.75$-ML precovered surface are shown in Fig. 3. There is a noteworthy shift to higher E_{trans} with increasing rotational energy, which was also observed for $v=1$ molecules. In contrast, no shifts with rotational energy are observed for NO ESD from the clean surface.[16]

Finally, we note that all of the E_{trans} distributions discussed above correspond to the $\Omega=\frac{3}{2}$ spin-orbit level of the NO electronic ground state ($^2\Pi_{\Omega=3/2,1/2}$). Similar distributions were observed for the $\Omega=\frac{1}{2}$ level, as shown in Fig. 4. The major difference between the two *normalized* distributions is below the peak, where there is a broadening at low energy for the $\Omega=\frac{1}{2}$ population. It is important to note, however, that the *absolute yields* for both spin-orbit levels at the lowest E_{trans} are the same within experimental error. In contrast, in nonthermal laser-induced desorption (LID), E_{trans} distributions for the $\Omega=\frac{3}{2}$ NO desorbate peaked at higher energies than the $\Omega=\frac{1}{2}$ distributions.[13,35]

B. NO yield versus O coverage

The specific NO ($v=0$) ESD yield increases exponentially with oxygen atom coverage (Θ_O) on Pt(111), as is shown in Fig. 5. The increase is much greater for the $^2\Pi_{3/2}$ spin-orbit state, which is roughly 120 cm^{-1} above the $^2\Pi_{1/2}$ ground-state level.[36] The specific yield for each spin-orbit state at a given Θ_O was calculated by first integrating over each E_{trans} distribution (discussed above), then normalizing the result to that coverage of saturation NO. The latter was found previously[3] to be 0.5–0.6 ML on the clean surface and inversely proportional to Θ_O with a slope of $-\frac{1}{2}$; thus at $\Theta_O=0.75$ ML, the saturated NO coverage is 0.15 ML.

At 350-eV electron-beam energy, the yield was close to its maximum. However, an appreciable fraction of the yield could be attributed to secondary electrons.[37,38] With this in mind, the increase in NO desorption cross section γ at 350 eV due to the presence of coadsorbed O can be estimated. On the clean surface, $\gamma\simeq 6\times 10^{-19}$ cm^2 for the NO populations at the $v=0$ P_{12} ($\Omega=\frac{3}{2}$) and P_{11} ($\Omega=\frac{1}{2}$) band heads ($J=9.5-11.5$). This is calculated from the 2×10^6 molecules/cm^3 density of neutral particles in the laser beam area under the conditions of a 350-eV electron-beam fluence of 1.6×10^{16} electrons/cm^2 s, an NO coverage of 7.5×10^{14} molecules/cm^2, and an average NO velocity of 5×10^4 cm/s. Since the electron-beam area on the surface is ~ 0.016 cm^2, the flux density of particles in the laser beam is assumed to be reduced by a factor of 31 (0.5 cm^2/0.016 cm^2) relative to the density leaving the surface. At $\Theta_O=0.75$ ML, the enhancement in *specific* yield for the sum of the $^2\Pi_{3/2,1/2}$ spin-orbit values relative to the clean surface is about 90 ± 6 for the same excitation conditions. Since this value has already been corrected for the increased velocity exhibited at $\Theta_O=0.75$ ML, the NO ($v=0$, $J=9.5-11.5$) cross section γ is approximately 5×10^{-17} cm^2 for the coadsorbed system. The *total* neutral NO ESD cross section is higher, since it must include all vibrational and rotational levels.

The desorption cross section is comparable to the 6.4-eV LID cross section of NO from NiO (2×10^{-17} cm^2),[13] but about five orders of magnitude greater than the 3-eV LID cross section of NO from clean Pt(111).[35] Since the flux of desorbing molecules during the electron pulse was still only $\sim 10^{14}$ molecules/cm^2 s from the $\Theta_O=0.75$-ML surface, desorbate collisions above the substrate were

negligible. In fact, this value is seven orders of magnitude below the onset of expected collisional distortions.[39] Erosion of the surface layer was a concern, however, but not a serious one since a 350-eV, 1.0-μs pulse desorbs $\sim 10^{-7}$ monolayer.

C. Site dependence of NO ESD yield on clean Pt(111)

One of the interesting features of NO chemisorption on *clean* Pt(111) is the population of two adsorption sites: bridge and atop.[3,27] At low NO exposures [<0.3 L (1 L $=10^{-6}$ Torr s)], the bridge site is favored, but at the highest exposures as used here (saturation), the atop sites are more populated.[27] The LID of NO from Pt(111) (Ref. 35) was attributed exclusively to NO adsorbed on atop sites. Earlier, Nezter and Madey found that ESD of NO^+ from Ni(111) derived from atop sites.[40] In the present work, it is clear from Fig. 5 that the O-induced yield enhancement increased exponentially well beyond $\Theta_O=0.25$ ML, the coverage at which no bridge sites were occupied by NO.[3] Thus any conversion of bridge to atop sites was definitely not the sole basis for these observations.

In order to see if site conversion plays any role in the ESD yield of neutral NO from Pt(111), desorption from the *clean* surface was examined when atop-bound NO molecules were selectively removed, as illustrated in Fig. 6. (A similar method was used by Buntin *et al.*[35].) In the middle of the figure is shown the TDS of NO from the Pt(111) surface saturated with NO at 100 K (hence the presence of the 200-K peak which was not allowed to form in data-acquisition runs). Thermal desorption from atop sites (β_1) commences at $T=300$ K, followed by desorption from the bridge sites (β_2) at $T>350$ K. If a saturated surface is annealed at 300 K, then all the atop-bound NO are either desorbed or converted to bridge-bound species.[3,27] A TDS from the "bridge-only" surface prepared this way and allowed to cool back to 90 K is shown at the bottom of Fig. 6. It was found that the specific $v=0$ yields and the TOF E_{trans} distributions for both $^2\Pi_{3/2,1/2}$ spin states were the same for the bridge-only surface relative to the regular saturated surface which has mostly atop NO. Thus there appears to be no difference, within experimental error, in the stimulated desorption cross section or E_{trans} distributions from the two sites on the clean surface.

D. Threshold for NO ESD from O-covered Pt(111)

The ESD thresholds for the $v=0$, 1, and 2 vibrational levels of NO ($^2\Pi_{3/2}$) from the $\Theta_O=0.75$-ML precovered Pt(111) substrate are shown in Fig. 7 for a fixed E_{trans} window of 0.15–0.27 eV. If we assume that the final states of the primary electron and the excited adsorbate electron(s) are at the Fermi level, then the surface excitation energy is given by $E_{HV}+\phi_C$, where ϕ_C is the 4.1-eV work function of the electron-gun cathode. Thresholds for all three vibrational levels are approximately 9–10 eV for *both* clean and O-covered surfaces. It is important to note that there is a complete absence of a "peak" centered at 12 eV which was previously observed for NO ESD from the clean surface.[15] We now know from background scans (Sec. II) that the peak was derived from ESD of NO from the crystal supports and was thus spurious.

E. Internal energies of NO ESD from O-covered Pt(111)

1. $\Omega=\frac{3}{2}$ spin-orbit propensity

The electronic ($\Omega=\frac{3}{2},\frac{1}{2}$), rotational, and vibrational energy distributions of ground-state NO desorbed from $\Theta_O=0.75$-ML precovered surface were obtained for a fixed excitation energy of 350 eV and TOF delay time corresponding to a $E_{\text{trans}}=0.15$–0.27-eV window. Since the rotational spectra were dominated by the $\Omega=\frac{3}{2}$ spin-orbit propensity, this effect will be discussed first. On the clean surface there was no propensity (the $\Omega=\frac{3}{2}$ and $\frac{1}{2}$ populations were equal). In Fig. 8, the specific-yield data of Fig. 5 are replotted as the relative yield

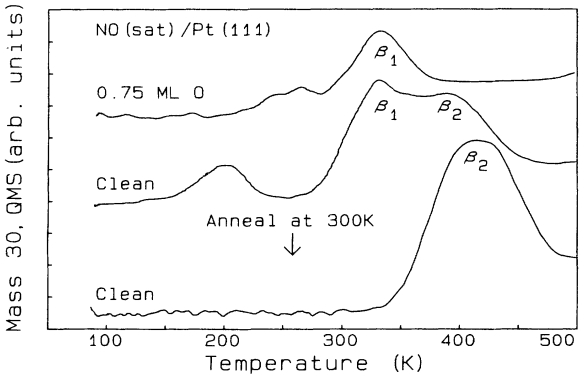

FIG. 6. Thermal desorption of NO from a $\Theta_O=0.75$-ML precovered Pt(111) surface (top) and from a clean Pt(111) surface (middle). The bottom curve shows the NO thermal desorption from a saturated NO layer on the clean surface which was annealed at 300 K to drive off atop NO. The β_1 and β_2 peaks refer to desorption from atop and bridge sites, respectively.

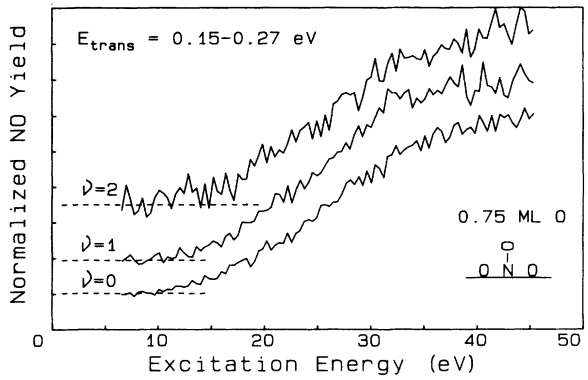

FIG. 7. Normalized, unsmoothed, ESD thresholds for the $v=0,1,2$ levels of NO from a 0.75-ML O-covered Pt(111) surface. The delay time and electron-beam pulse width (1 μs) were such that the window of $E_{\text{trans}}=0.1$–0.27 eV. The dashed base lines have been shifted up from zero for display purposes.

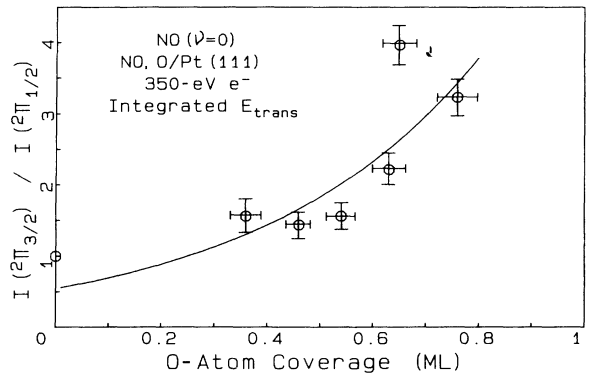

FIG. 8. $^2\Pi_{3/2}$ propensity vs oxygen-atom coverage (Θ_O). The $I(^2\Pi_{3/2})/I(^2\Pi_{1/2})$ ratios were calculated from the integrated TOF data given in Fig. 5, while the best-fit curve was obtained by the ratio of the respective exponential curves in Fig. 5.

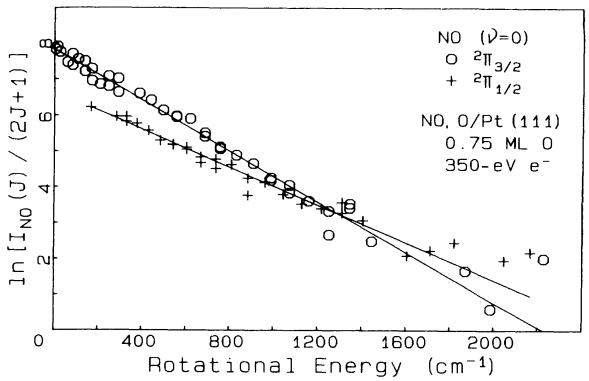

FIG. 10. Rotational energy (E_{rot}) distributions of the $^2\Pi_{3/2,1/2}$ NO ($v=0$) spin-orbit levels desorbed by 350-eV electrons from the $\Theta_O=0.75$-ML covered Pt (111) surface.

$I(^2\Pi_{3/2})/I(^2\Pi_{1/2})$ vs Θ_O. One can see that the $\Omega=\frac{3}{2}$ propensity becomes apparent at $\Theta_O>0.4$ ML and increases with oxygen coverage to a maximum of ~ 3.5. The latter is similar to the $\Omega=\frac{3}{2}$ propensity of ~ 3 for the LID of NO from *clean* Pt(111), where *no* propensity was observed in the ESD.

The $\Omega=\frac{3}{2}$ propensity is clearly maximum at the lowest NO rotational energy, as shown in Fig. 9, where J is the half-integral angular momentum quantum number. Some of the propensity was lost at high J because of mixing of the pure Hund's case (a) wave functions for the $\Omega=\frac{3}{2}$ and $\frac{1}{2}$ levels due to the spin-uncoupling operator.[32] However, as will be discussed in Sec. IV C, the observed loss in propensity versus J was considerably greater than that expected by this mixing.

2. *Rotational energy*

The rotational energy distributions for the NO $^2\Pi_{3/2,1/2}$ $v=0$ spin-orbit levels are shown in Fig. 10. To derive an "average" rotational energy, the slope of the best-fit line for $\ln[I_{NO}(J)/(2J+1)]$ versus rotational energy is determined. In order to do this independent of the $\Omega=\frac{3}{2}$ and $\frac{1}{2}$ populations, the spin-orbit populations were summed at each rotational quantum number from the individual $\Omega=\frac{3}{2}$ and $\frac{1}{2}$ best-fit lines. For the $v=0$ data in Fig. 10, the result is a rotational energy of 449 ± 18 K.

For the $v=1$ and 2 levels, the same $\Omega=\frac{3}{2}$ propensity of ~ 3.5 was observed at the band heads. However, due to the reduced $v=1,2$ yield, not enough $\Omega=\frac{1}{2}$ lines were resolved to calculate a spin-orbit sum as per the $v=0$ data. In these cases, only the $\Omega=\frac{3}{2}$ spectra for the $v=1,2$ levels can be plotted as in Fig. 9 and a best-fit line determined. If one assumes that the propensity $I(^2\Pi_{3/2})/I(^2\Pi_{1/2})$ in the $v=1,2$ levels has the same J dependence as that in Fig. 10, then the $\Omega=\frac{1}{2}$ intensities can be extrapolated and summed with the $\Omega=\frac{3}{2}$ data. The average rotational energies estimated in this manner for the $v=1,2$ vibrational levels are 531 ± 37 and 501 ± 50 K, respectively.

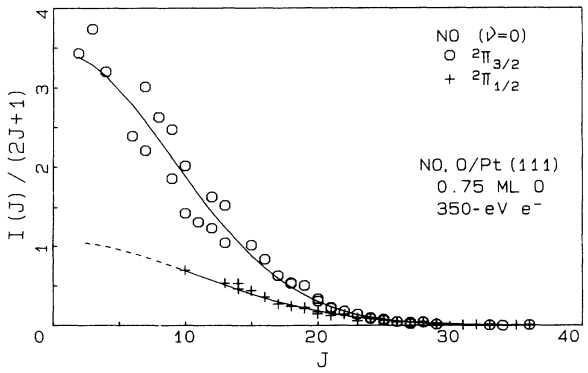

FIG. 9. $^2\Pi_{3/2}$ and $^2\Pi_{1/2}$ intensities normalized by the degeneracy factor $(2J+1)$ vs rotational quantum number J for NO ($v=0$) desorbed by 350-eV electrons from the $\Theta_O=0.75$-ML covered Pt(111) surface. The solid lines are the least-squares best-fit curves from each data set. The dashed curve is an extrapolation of the $^2\Pi_{1/2}$ best fit to low J.

TABLE I. Energies of NO products.

v	Population	E_{trans} peak (eV)[a]	E_{rot} (K)
	NO ESD from clean Pt(111)[b]		
0	1.00	0.05	543±54
1	0.58±5%	0.05	581±58
2	0.26±5%	0.05	642±64
3	0.43±5%	0.05	481±60
	NO ESD from 0.75 ML O precovered Pt(111)		
0	1.00	0.18	449±18
1	0.38±5%	0.18	531±37
2	0.21±5%	0.18	501±50
3	not detected		

[a]TOF maxmum on an energy scale.
[b]From Ref. 15.

3. *Vibrational distributions*

The population distribution over the observed vibrational levels was obtained by summing all the best-fit rotational lines for each level out to 1000 cm^{-1} (the detection limit for $v=2$). From this procedure, the vibrational distribution was estimated to be (1.0):(0.38):(0.21) for $v=0$, 1, and 2, respectively. Higher vibrational levels were not detected. The vibrational distribution and rotational energies for the ESD of NO from the $\Theta_O=0.75$-ML precovered Pt(111) surface are summarized at the bottom of Table I. When compared with the internal energies of the NO ESD from the clean surface, there appears to be a distinct decrease in NO internal excitation from the oxygenated surface.

IV. DISCUSSION

The most dramatic effects of coadsorbed O on the ESD of NO from Pt(111) are a large yield enhancement and a pronounced propensity for the desorption of NO molecules into the $^2\Pi_{3/2}$ (upper) spin-orbit level. Other effects observed are a shift in the E_{trans} distributions to higher energies and decreases in the internal vibrational and rotational energies. The only aspect of the process that has *not* changed with the presence of oxygen is the threshold energy; we correlate the threshold to the creation of a hole in the 5σ molecular orbital of the NO adsorbate. Thus we begin our discussion with the electronic structure of the adsorbate-metal system (Sec. IV A). We find that the changing yield, translational energy distributions, and vibrational energies can be understood in terms of an oxygen-induced reduction in charge transfer from the substrate into the adsorbate 2π molecular orbital. This charge screens the desorption-producing electronic excitation; the change in charge-transfer screening and the consequences are discussed in Sec. IV B.

Given that the adsorbate is temporarily ionized after the Auger decay of the excited state, the adsorbate must be reneutralized using electrons from the strongly spin-orbit-split Pt(111) substrate. If, in addition, the excited adsorbate is aligned along the surface normal due to a rotationally hindering potential, then the neutralization rate into the $\Omega=\frac{3}{2}$ level is greater than that into the $\Omega=\frac{1}{2}$ level. This results in the observed spin-orbit propensity in the desorbate, as discussed in Sec. IV C. Finally, in Sec. IV D we will qualitatively discuss factors leading to the rotational and translational energy distributions. Thus we see there are basically four aspects which explain our observations: (a) the desorption producing excitation, (b) charge-transfer screening of the excitation, (c) neutralization of a hindered-rotor adsorbate by a strongly spin-orbit split substrate, and (d) dynamics on the excited-state potential.

A. Electronic structure and the $5\sigma^{-1}$ desorption channel

The energy-level diagram of NO adsorbed on Pt(111) is shown schematically in Fig. 11. On the far left of the figure, the Pt valence bands stretch roughly from the Fermi level E_F (our zero of energy) to approximately 7 eV below.[3,41] The NO energy levels in the middle of the

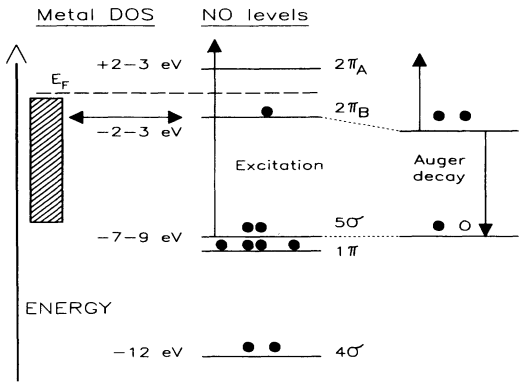

FIG. 11. Electronic energy-level diagram of NO/Pt(111) chemisorption. Excitations are screened by the metal through the 2π bonding level, and intramolecular Auger decay of excitations deeper than 7 eV occur through the $2\pi^2$ configuration (right).

figure have been mapped out by UPS.[3,42] According to one-electron theory, interaction between the singly occupied 2π orbital of the NO and the near degenerate Pt $d\pi$ valence levels rehybridizes the 2π into adsorbate bonding ($2\pi_B$, below E_F) and antibonding ($2\pi_A$, above E_F) levels. The unoccupied $2\pi_A$ level has been observed in inverse photoemission spectra.[43] The splitting of the molecular 2π level indicates a substantial 2π-metal interaction; thus excitations involving 2π resonances (e.g., $2\pi_B \rightarrow 2\pi_A$, $d\pi \rightarrow 2\pi_A$) will be very short lived due to efficient tunneling to and from the substrate. These excitations are low-probability desorption channels, hence the small cross section for 3-eV ($d\pi \rightarrow 2\pi_A$) LID of NO from Pt(111).[35]

The 9–10-eV threshold for NO ESD from both clean and O-covered surfaces corresponds well with excitation of the adsorbate 5σ or 1π electrons. The 1.5-eV increase in binding energy[3] of these levels on the $\Theta_O=0.75$-ML surface relative to the clean surface is not observed in the thresholds due to low signal level. Most important is that the 5σ and 1π levels are not degenerate with the metal valence bands; thus holes in these levels cannot decay by resonant tunneling, and necessarily must Auger decay. Since intra-atomic is much faster than interatomic Auger decay,[44] the dominant decay channels, for both $5\sigma^{-1}$ and $1\pi^{-1}$ excitations, use two 2π electrons. The $1\pi^{-1}$ channel has a much shorter lifetime than the $5\sigma^{-1}$ because the $1\pi^{-1}$ Auger decay rate is not inhibited by an exchange of angular momentum between the two 2π electrons.[15,19] Similarly, deeper excitations are expected to decay rapidly via shallower levels of the same symmetry (e.g., a 4σ hole filled by a 5σ electron). In general, longer-lived excitations will dominate the desorption process; thus we have assigned the primary channel to a 5σ hole.[15,19] The desorption of neutral CO from clean and Cu-covered W(110) also has revealed a long-lived $5\sigma^{-1}$ channel.[45] Finally, given the intimate role of the 5σ electrons in reducing the repulsion between the N and Pt ion cores in the NO-Pt σ-donation (or electrostatic) bond,[46,47] it follows that a $5\sigma^{-1}$ excitation will result in a

repulsive force between the molecule and the surface.

It is consequential that apparently the long-lived two-hole $5\sigma^{-2}$ excitation on the O-covered surface does not significantly contribute to the desorption yield. This is evident by the absence of any structure at $\sim 18-20$ eV in the threshold data. The $5\sigma^{-2}$ channel is, however, most likely responsible for the high-energy peak in the $v=2,3$ E_{trans} distributions (mentioned in Sec. III A) for neutral NO desorption from the *clean* surface;[15] it is also the dominant channel for neutral CO desorption from Pt(111) (Ref. 15) and Ru(001).[48]

B. Charge-transfer screening and the enhanced ESD yield

Auger electron energies associated with O(1*s*) core hole decay in CO on Ni(111) and on Ru(001) indicate strong 2π screening of two-hole states, made possible by significant adsorbate-substrate interaction.[49,50] We expect 2π screening of NO one-hole and two-hole excitations on Pt(111) to be similar. Since the 2π orbital is molecularly antibonding, N-O bonds are weakened by chemisorption involving metallic "backbonding" into the 2π.[46] It can be inferred from HREELS (Ref. 3) that coadsorbed O on Pt(111) reduces the NO backbonding: there is an increase in the N-O bond stretching frequency along with a decrease in the NO-surface stretch, relative to the clean surface. Since the NO ground state apparently has less 2π charge in the presence of O, it follows that there should likewise be an O-induced reduction in the 2π screening charge for one-hole excitations. In this section, we focus on the change in charge-transfer screening of excitations produced by the presence of coadsorbed oxygen and see how the $5\sigma^{-1}$ lifetime and desorption yield are affected.

There are, however, three other effects due to the presence of oxygen which might cause a change in the yield and thus should be addressed. One possibility is that a new desorption channel opens due to coadsorbed oxygen; however, the unchanged threshold eliminates all but the $1\pi^{-1}$ as a new channel. Lifetime arguments discussed in Sec. IV A essentially rule this possibility out. Only in the event of near-zero 2π occupancy would the 1π hole be longer lived than a 5σ hole; this is because the 5σ hole has a larger *inter* atomic Auger rate due to larger orbital overlap with the metal. Near-zero occupancy is extremely unlikely, however, because the excited molecule would then have $+2$ charge ($5\sigma^{-1}2\pi^{0}$). Furthermore, if the 1π channel were to "turn on" in the presence of oxygen, we would expect *increased* rather than decreased vibrational excitation in the desorbates due to holes in the strongly bonding 1π orbital. *Thus we conclude that the $5\sigma^{-1}$ excitation dominates desorption both with and without oxygen present.*

A second possibility is a larger localization probability. In order for desorption to occur, the excitation must localize (self-trap) on a single adsorbate.[51] Our previous analysis of the coverage dependence of NO ESD from clean Pt(111) concluded that, at high NO coverages, most $5\sigma^{-1}$ excitations do not localize.[16] The presence of oxygen serves to space the NO molecules and thus reduce the $5\sigma^{-1}$ bandwidth. This should enhance self-trapping and consequently increase the desorption probability. However, our previous data show that this effect can only increase the desorption cross section by about a factor of 6,[16] which is still a factor of 15 too small. Thus we conclude that self-trapping plays only a minor role in the coadsorbate effects.

A third possibility is a change in desorption yield due to substantial changes in the dynamics of the desorption process. By "dynamics" we mean that the ground- and/or excited-state potential-energy surfaces are altered by the presence of oxygen so that nuclear wave-packet evolution is significantly changed. Thermal desorption and HREELS data show that ground-state binding energies and adsorbate frequencies are only mildly affected by oxygen coadsorption.[3] Thus we do not expect sizable changes in the desorption probability due to changes in the ground-state potential. The excited-state potential is undoubtedly changed by the presence of oxygen; however, the oxygen is not expected to greatly change the 5σ-electron density between the N and Pt ion cores, and hence should not significantly change the respulsive force. If the repulsive force in the excited-state at the ground-state equilibrium position did increase, we would, on one hand, expect a higher probability for desorption, but, on the other hand, we would also expect a concomitant change in the *width* of the E_{trans} distribution. This follows from the fact that a larger force implies a shorter time for the desorption event and thus a broader translational energy distribution. Figure 1 clearly shows little change in the width of the distribution. We therefore conclude that dynamics is probably not at the heart of the increased yield.

Thus we find only one reasonable candidate capable of simultaneously explaining several of our observations: a change in the lifetime of the 5σ hole due to a reduction in the 2π screening. Such a situation causes several things, even in the absence of changes in the ground- or excited-state potential energy surfaces: (1) the translational energy should increase due to increased time for acceleration in the excited state; (2) the NO excited vibrational populations should decrease due to a reduction in excited-state antibonding 2π occupancy; and (3) since most excitations decay before sufficient acceleration occurs to produce desorption, we expect exponential dependence of the neutral yield on lifetime. The observation of all three trends strongly suggests that the lifetime of the primary excitation monotonically increases with oxygen coverage. We will now show that the coadsorbed oxygen changes the 2π electron density sufficiently to explain the giant yield enhancement. As noted above, the yield is expected to have exponential dependence $\exp(-\tau_c\Gamma)$ on the characteristic or "critical" time τ_c for desorption[8] and the $5\sigma^{-1}$ lifetime Γ^{-1}. Assuming $\tau_c > 1/\Gamma$, we expect that lifetime changes of roughly 1.5–3 would account for the enhanced yield.

The $5\sigma^{-1}$ Auger decay rate scales as the square of the amplitudes C_n of the contributing $2\pi^n$ configurations in the excited-state wave function $\Psi^* = \sum_{n=0}^{4} C_n \chi^*(2\pi^n)$, where $\chi^*(2\pi^n)$ is the configuration wave function of the adsorbate with $n\,2\pi$ electrons and a 5σ hole. Since a 5σ

hole uses two 2π electrons in the dominant Auger channel, only the $2\pi^n$ configurations where $n \geq 2$ contribute significantly to the rate. No appreciable contributions come from $2\pi^1$ or $2\pi^0$ since one or two metal electrons must be used and interatomic Auger rates are much slower. Since the $2\pi^4$ and $2\pi^0$ configurations are too high in energy, Ψ^* is dominated by the $2\pi^1$, $2\pi^2$, and $2\pi^3$ configurations ($|C_1|^2+|C_2|^2+|C_3|^2 \approx 1$). In addition, since the $2\pi^2$ and $2\pi^3$ configurations have approximately the same Auger rates, the relative decay rate scales as $\Gamma \propto (1-|C_1|^2)$.

Oxygen can reduce 2π backbonding in several ways, such as by direct through-space electrostatic interactions and by changing the work function ϕ. The severity of the work-function dependence is due in large part to the weakness of the $d\pi$-2π covalent portion of the substrate-adsorbate bond, the relative neutrality of the excited molecule in the absence of oxygen, and the proximity in energy of the positive, neutral, and negative configurations in the excited state. We argue below that these conditions are met by this system.

Recent *ab initio* calculations by Pacchioni and Bagus[47] for CO/Pd(100) found considerably more π backbonding than occurs in first-row elements. They also found that the greatest cause of chemisorption-induced change in the C-O vibration was backbonding charge transfer, but that only a fraction of the binding energy was from this source. Due to similarities in the $d\pi$-2π orbital for NO/Pt(111), we anticipate similar conclusions. We assume that about half of the ~ 1.0-eV Pt-NO binding energy is due to $d\pi$-2π interaction and that $\sim \frac{1}{3}$ electron is transferred to NO in the ground state. The above-mentioned Auger experiments[49,50] on chemisorbed CO suggest facile charge-transfer screening in the two-hole excited state, in that the screened hole-hole interaction (U) is small (<2 eV). If we assume that this also applies to single-hole excited states of NO on Pt(111), excited ($5\sigma^{-1}$) NO is approximately neutral (i.e., is well screened). Since U also reflects the differences in energy of the charged and neutral configurations, $U=[E(+)-E(0)]+[E(-)-E(0)]$, these experiments also suggest a proximity in energy on the clean surface.

The role of the oxygen is transparent: the work function ϕ increase lowers the energy of the positive excited-NO configuration ($2\pi^1$) while raising, by the same amount, the energy of the negative configuration ($2\pi^3$) relative to the neutral configuration ($2\pi^2$). Since the $d\pi$-2π bond is weak (~ 0.5 eV), a $\Delta\phi$ of $+0.5$ eV changes each of these energies by an amount comparable to the magnitude of the off-diagonal matrix elements which mix these configurations and create the $d\pi$-2π covalent bond. Because of near neutrality on the clean surface and the proximity in configuration energies, $\Delta\phi$ is also comparable to the small diagonal energy differences. Thus the resulting $2\pi^n$-configuration amplitudes are necessarily very sensitive to $\Delta\phi \sim 0.5$ eV, given that other energies in the problem do not change. We would expect similar results in any weakly chemisorbed system where lifetime largely depends on the filling of a partially occupied orbital. Indeed, analogous effects have been recently observed in the stimulated dissociation of NO_2 coadsorbed with O on Pt(111).[52]

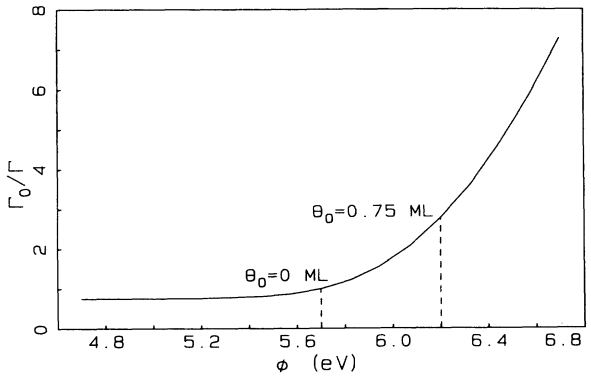

FIG. 12. The relative $5\sigma^{-1}$ excitation lifetime in adsorbed NO is plotted vs substrate work function. The lifetime is normalized to unity at the work function of the clean Pt surface (Ref. 3), as indicated. The work function of the substrate with $\Theta_O=0.75$ ML is also indicated (Ref. 3).

Since the Auger decay rate scales as $\Gamma \propto (1-|C_1|^2)$, we expect a decreased rate with increasing ϕ. Figure 12 shows the numerical results of relative Auger lifetime Γ_0/Γ vs ϕ, where $\Gamma_0/\Gamma=1$ for the clean surface ($\phi=5.7$ eV). The lifetime change shown is not without bound, however. For lifetimes greater than $10\times$that of the excited neutral molecule, contributions from interatomic channels which use a metal electron directly cannot be neglected. Interatomic channels will thus cause the effect to saturate at high work functions and/or high direct electrostatic interactions which make the molecule positive in the excited state. However, we have shown that the exponential dependence of yield on lifetime, coupled with the quadratic dependence of lifetime on wave-function amplitude, makes ESD an extremely sensitive probe of coadsorbate-induced rehybridization.

C. Spin-orbit propensity

Our observation of a spin-orbit propensity of $^2\Pi_{3/2}$:$^2\Pi_{1/2} \approx 3.5$ is very reminiscent of a similar observation in LID of NO from atop sites on clean Pt(111).[35] In that experiment, 3-eV photons are believed to produce "hot" electrons which are captured into the short-lived $2\pi_A$ antibonding resonance. In addition to the small LID yield ($\sim 10^{-4}$–10^{-6} that of ESD), the translational energy distributions differ for the two spin-orbit states, the hotter one being $\Omega=\frac{3}{2}$. In contrast, the ESD spin-orbit translational energy distributions are virtually the same (Fig. 4). Finally, LID desorbates are rotationally and vibrationally cold relative to ESD. Thus there are more differences than similarities in these two experiments, but nonetheless, the same propensity is observed. We adopt the philosophy that the propensity in the two experiments is related.

It has been suggested[13,35] that the calculations of Smedley, Long, and Alexander[53] for NO scattering from a flat surface might be relevant; i.e., the propensity is the result of a quantum-mechanical interference effect for scattering on two ground-state potential-energy surfaces which are degenerate only at the surface normal. We

disagree with this proposal for the simple reason that Smedley, Long, and Alexander investigated a very different physical process: an initially prepared cold (low J, $\Omega=\frac{1}{2}$) NO molecule collides with the surface and scatters into higher J and *both* spin-orbit states. In contrast, the desorption experiments begin with a hot (many J), mixed spin-orbit initial state. It is difficult to imagine subtle quantum-dynamics interference effects would be able to unmix them. We argue below that the propensity is due instead to the transfer of an electron from the strongly spin-orbit-split Pt(111) substrate of the open-shell NO desorbate.

In order to understand the origin of the spin-orbit propensity it is first necessary to have an understanding of the angular momentum of the NO molecule. Because of the open-shell nature of this diatomic, there are two good quantum numbers for each vibrational state for which population distributions are experimentally measurable: total angular momentum and spin orbit. The total angular momentum J is the vector sum of three components $j+L+S$, where j is the rotor momentum, L is the orbital angular momentum about the center of mass of the molecule of the single electron in the 2π orbital, and S is its spin angular momentum.[54] The magnitudes of J and S are conserved, but those of j and L are not. However, the projection of $L(\Lambda)$ onto the molecular axis is approximately conserved and is ±1, and the projection of $S(\Sigma)$ is $\pm\frac{1}{2}$. Since the projection on the molecular axis of the rotor momentum j is always zero, the magnitude of the projection (Ω) onto the axis is $\frac{1}{2}$ or $\frac{3}{2}$. The spin-orbit quantum number is related to this projection. In the limit of Hund's case (a),[32,54] the projection is the good quantum number; however, NO crosses from Hund's case (a) to Hund's case (b) with increasing J. The spin-orbit states are coupled (fixed J, different Ω) by the Hamiltonian with matrix element $h_{1/2,3/2;J}=-B[(J-1/2)^2-1]^{1/2}$ (Ref. 54) for $J\geq 3/2$; whereas the difference in energy between them is $A-2B$ where A is the spin-orbit parameter [~ 119 cm^{-1} for NO (Ref. 36)] and B is the rotational constant [~ 1.67 cm^{-1} for NO (Ref. 36)]. Since $A\gg B$, this is a Hund's case (a) diatomic for moderate J's. In particular, the lower spin-orbit level is 90% pure $\Omega=\frac{1}{2}$ at $J=25.5$.

We now consider spin-orbit splitting in the Pt substrate because it is our hypothesis that this is the origin of the observed propensity. In particular, we contend that the angular momentum projection of electrons with energies near E_F onto the (111) normal is pertinent. The significance of E_F arises because the neutralizing electrons in ESD must be close to it to be resonant with the 2π level of NO (or even an excited NO level); and in LID, the hot electrons must arise near E_F because the laser excitation energy is rather low. The significance of the projection along the normal is that this is the preferred neutralization axis by the nature of being the shortest distance from the metal to the temporary ion. Recall that in ESD the desorbate is ionized in the Auger decay of the excited state. In LID the normal is the axis for hot-electron transfer onto the molecule (assuming the molecule is not appreciably bent).

Group-theoretic arguments predict[55] that with circularly polarized light, photoemitted electrons from a strongly spin-orbit split substrate should be spin polarized. In normal incidence, normal takeoff photoemission from Pt(111) with 13-eV circularly polarized light,[56,57] the observed polarization near E_F is indeed 50%, or 3:1. Furthermore, electrons with $m_j=\frac{3}{2}$ cannot mix with those of $m_j=\frac{1}{2}$ since they transform with different group representations in the C_{3v} double group. [This is the relevant point group for a spin-orbit split (111) surface at an atop site.] The experiment, together with theoretical details,[55,58] unequivocally determines that, along the normal the top-most Pt(111) band which crosses E_F is $m_j=\frac{3}{2}$ and not $m_j=\frac{1}{2}$. Hence we conclude that there are ~ 3 neutralizing electrons with $m_j=\frac{3}{2}$ to every one with $m_j=\frac{1}{2}$.

A different density of states for $m_j=\frac{3}{2}$ than for $m_j=\frac{1}{2}$ along the surface normal does not in itself guarantee a propensity in the neutralization. However, if the NO desorbate is *aligned along the surface normal and above an atop site* at the time of reneutralization, then the propensity would reflect the substrate density of states. The atop site is in fact the only binding site when oxygen is present, and in LID it has been shown that the stimulated desorbates also come exclusively from atop sites. It should be noted, however, that there is some evidence that on the oxygenated surface, ground-state NO is tilted[3] and not aligned normal as on the clean surface. We believe the observed propensity indicates that the desorbate does leave the surface oriented along the normal. Thus, if the ground state is indeed tilted, possibly the excited state serves to reorient the desorbate. In fact, this leads to the prediction that angle-resolved ESD will show a distribution that peaks on normal. Experiments are currently underway to verify this.

This argument for a propensity is rigorous from symmetry alone. The magnitude and the direction of the propensity is inferred from the circularly polarized photoemission experiments. Thus we propose that the ESD excited-state potential is hindered due to a steric and/or electronic effect of the coadsorbed oxygen. Previously we claimed that on the clean surface the excited-state potential is likely to be a free rotor, consistent with the absence of any observed spin-orbit propensity and with the independence of the translational energy distributions on the rotational quantum number. On the oxygenated surface, however, the translational energy distributions are no longer independent of rotational quantum number. This is consistent with a hindered rotor excited state and is discussed further in Sec. IV D.

We now come to the observation of a loss or dilution of the spin-orbit propensity observed in ESD as a function of J (Fig. 9) with fixed E_{trans}. Since the desorbate is not completely aligned along the normal, it is not *a priori* obvious that the neutralization rate into the different spin-orbit states is J independent. Consequently, we have calculated the neutralization rate of a rotating, but *non-translating*, hindered rotor. We assumed a wave function with a distribution in angle from the normal similar to the ground state with the experimental hindered rotor

frequency of 510 cm^{-1},[3] but an expected value for the rotational energy taken from the measured desorbate distribution of 450 K from Table I ($v=0$). This rotational energy is significantly hotter than the ground-state hindered rotor (Sec. IV D). The calculation includes the coupling between the two spin-orbit states, as mentioned above. The decay of the propensity with J due to the mixing operator should be $[1+(F-1)\cos^2\theta_J]/[1+(F-1)\sin^2\theta_J]$, where F is the propensity and θ_J is the mixing angle $\{\tan 2\theta_J = 2B[(J-1/2)^2-1]^{1/2}/(A-2B)\}$. Our calculation showed effectively no decay of propensity with J in the absence of the coupling operator. With $F=3$ (4) and $J=15.5$ the propensity is expected to be 2.7 (3.5) or only a 10% (13%) dilution; nevertheless, a 50% dilution is observed. Thus further study is required to understand the dilution of the propensity with increasing rotational energy. One obvious shortcoming of this calculation is the nontranslating desorbate, and also the uncoupling of translation and rotation. The translational energy distributions do indicate a weak coupling observed at high J (Fig. 3). In additional, the propensity is lost for desorbates with the lowest velocities (<0.15 eV) and relatively low rotational content (Fig. 4). This loss of propensity for slowly moving desorbates could be the result of residual interactions with the substrate after neutralization.

What about the LID experiments? A further consequence of the C_{3v} double group and a larger $m_j=\frac{3}{2}$ (aligned) relative to $m_j=\frac{1}{2}$ (antialigned) density of states to interact with the NO molecule is that along the normal there must be two nondegenerate bonding as well as antibonding potential-energy surfaces due to the interaction of the NO 2π and Pt $d\pi$ orbitals. The NO 2π orbitals are very nearly degenerate, whereas the Pt $d\pi$ orbitals are split by the large spin-orbit coupling in Pt, $d\pi$ aligned being higher in energy than $d\pi$ antialigned. Thus, assuming that the 2π level is more nearly degenerate with $d\pi$-aligned orbitals, then the aligned $d\pi$-2π bond would be a stronger bond that the antialigned $d\pi$-2π bond. Similarly, the aligned antibonding level should be more repuslive than the antialigned antibonding level. Crudely speaking, the hot electron (3:1 $m_j=\frac{3}{2}$:$m_j=\frac{1}{2}$) gets captured into the antibonding resonance. In addition, the bonding state should have more $m_j=\frac{3}{2}$ than $m_j=\frac{1}{2}$ character. This could explain the observed propensity in the LID experiments as well as the observed difference in translational energy distributions for two different spin-orbit states. A final note is that the LID data indicate a strongly peaked desorption distribution about the surface normal,[35] consistent with our model.

To summarize our interpretation of the ESD results, the strongly spin-orbit split metal surface (with C_{3v} symmetry about each surface substrate atom) has a different and greater density of states (number of electrons) for $d\pi$-aligned ($m_j=\frac{3}{2}$) than $d\pi$-antialigned ($m_j=\frac{1}{2}$) electrons. Consequently, the resonant neutralization rate for aligned $NO^+ \rightarrow NO^0$ ($^2\Pi_{3/2}$) is faster than for $^2\Pi_{1/2}$. Providing the NO ESD desorbate is hindered at least to the point of reneutralization, the propensity is then expected. Furthermore, it is reasonable to believe that the coadsorbed oxygen causes the excited-state potential-energy surface to be hindered.

D. Dynamics on the excited-state potential

The dynamics of NO ESD from a clean Pt(111) surface has been considered previously.[15,19] Our best understanding can be briefly summarized as follows. The 2π-screened $5\sigma^{-1}$ excitation frees the hindered rotational motion of ground-state NO. Decay of the excitation thus finds some molecules in an orientation with respect to the surface which is different from the stable ground-state equilibrium geometry (normal to the surface with the N end down). The desorption probability increases considerably when excited NO has rotated more than about 15° from the normal. Since molecules that have higher rotational energies are more likely to have large deviations from normal and thus access weakly bound or unbound regions of the ground-state potential, there is an overall rotational "heating." However, the low E_{trans} distribution of the desorbed NO from the clean surface, together with the apparent finite probability for $E_{\text{trans}}=0$ (see Fig. 1), indicates that much of the kinetic energy acquired in the excited state is lost in overcoming the ground-state binding energy.

Unfortunately, we know little about the topography of the excited-state potential in the presence of the oxygen. Nonetheless, we presume it is repulsive along the surface normal at the equilibrium geometry of the ground state, and that the repulsive force is not overly sensitive to the presence of the coadsorbed oxygen. The increased lifetime, relative to that on the clean surface, of the $5\sigma^{-1}$ excitation in the presence of coadsorbed O enables the molecule to acquire more translational energy along the excited-state potential. The increased propagation time in the excited state also allows the excited molecules to decay further from the surface and thus access the weakest regions of the ground-state potential; this can be seen in the almost zero yield at the lowest E_{trans} in the $\Theta_O=0.75$-ML data (Fig. 1). However, unlike the dynamics on the clean surface, the observed spin-orbit propensity indicates that the excited state is hindered about the surface normal. Clearly the hindering must diminish as the molecule moves away from the surface; thus rotational and translational motion are necessarily coupled. Hasselbrink[59] has pointed out that in the presence of an anisotropic interaction with the surface as a function of orientation angle, rotational excitation can occur. That model has been used to explain the near-linear dependence of translational energies with rotational energies in LID experiments.[13,35,60] It is possible that we are seeing similar effects here, in that we observe higher than expected rotational energies and a shift (albeit, nonlinear) in E_{trans} with rotational energy (Fig. 3). No shift in NO E_{trans} with rotational energy was observed for the clean Pt(111) surface.[16] Thus the proposed anisotropy must be due to interactions with the neighboring oxygen atoms.

From both clean and oxygenated surfaces, we observe NO desorbates which are rotationally hot (400–600 K) relative to the available rotational energy from the ground-state hindered rotor. The ground-state NO-Pt

system has hindered rotor frequencies of ~465 (Ref. 61) and 510 cm^{-1} (Ref. 3) on clean and oxygenated (Θ_O=0.75 ML) Pt(111), respectively. In the harmonic-oscillator approximation, the zero-point energy is approximately half of the frequency and the zero point is divided equally between kinetic and potential energy. Thus the available energy is about $\frac{1}{4}$ the frequency or ~116 (clean) and 128 cm^{-1} (oxygenated). Both transalate to a relatively low rotational temperature of ~180 K. It is interesting to note that in the LID experiment, the desorbate rotational energy (~200 K) is close to this zero-point kinetic energy. However, LID is a very low probability event with a short lifetime, thus very little rotational excitation can occur in the excited state. In contrast, the lifetime in ESD is long enough for substantial excited-state dynamics resulting in rotational excitation. We argued above that for the clean surface, rotational heating is in part derived from the propensity for high over low rotor momentum desorption. In addition, there can be inelastic rotational scattering on the ground-state potential after deexcitation, since the molecules are deexciting close to the surface. We substantiated this heating with model calculations using a free-rotor excited state.[15] However, when the surface is oxygenated, we argued that the spin-orbit propensity derives from hindered desorbates. Thus the major source of rotational excitation for the NO desorbate on the oxygenated surface must be inelastic scattering on the excited-, the ground-state potential, or both.

V. CONCLUSIONS

The effects of coadsorbed oxygen atoms on the electron-stimulated desorption of NO from Pt(111) are varied and illuminating. Specifically we see, with increasing oxygen coverage, an exponential increase in the desorption yield, an increase in desorbate translational energy, a decrease in both vibrational and rotational energy, and a growing propensity for the upper spin-orbit level. In understanding these observations, a coherent picture of the dominant desorption process has emerged. A valence excitation is created in the adsorbate. Although the excitation is too deep in energy to decay into the metal valence band, it is screened almost instantaneously by the substrate through shallow, metal-absorbate rehybridized, levels. The excitation promotes atom motion on the excited-state potential and decays by a shallow valence Auger process, leaving a temporarily ionized desorbate. The latter must be resonantly reneutralized by the substrate, during which we contend the observed spin-orbit propensity is realized.

It follows that because the valence Auger decay uses electrons from the same orbital involved in screening the excitation, the lifetime, and hence the desorption yield from the dominant channel, is very sensitive to coadsorbate-induced changes in screening. Similar lifetime arguments should be applicable to enhanced ion desorption yields from higher energy, two-hole channels.[10] Vibrational excitation of the desorbate is also sensitive to the presence of screening charge since it occupies a strongly antibonding molecular orbital. Thus as the electronegative oxygen decreases the screening charge, the desorption yield increases while the desorbate vibrational excitation decreases. In conclusion, the exponential dependence of yield on excitation lifetime, coupled with the strong dependence of lifetime and internal state populations on the screening charge density, makes ESD a very sensitive probe of coadsorbate-induced rehybridization.

ACKNOWLEDGMENTS

The authors are indebted to T. Mayer for valuable comments. This work was supported by the U.S. Department of Energy under Contract No. DE-AC04-76DP00789.

[1]H. P. Bonzel, Surf. Sci. Rep. **8**, 43 (1987).
[2]M. E. Bartram, R. G. Windham, and B. E. Koel, Langmuir **4**, 240 (1988).
[3]M. E. Bartram, B. E. Koel, and E. A. Carter, Surf. Sci. **219**, 467 (1989).
[4]H. P. Bonzel, G. Pirug, and R. P. Messmer, Surf. Sci. **184**, L415 (1987).
[5]D. R. Jennison, J. Vac. Sci. Technol A **5**, 684 (1987).
[6]P. A. Schultz and R. P. Messmer, Surf. Sci. **209**, 229 (1989).
[7]P. A. Schultz, J. Vac. Sci. Technol. A **8**, 2425 (1990).
[8]D. Menzel and R. Gomer, J. Chem. Phys. **41**, 3311 (1964).
[9]*Desorption Induced by Electronic Transitions, DIET I,* edited by N. H. Tolk, M. M. Traum, J. C. Tully, and T. E. Madey (Springer-Verlag, New York, 1983).
[10]F. Bozso and P. Avouris, Chem. Phys. Lett. **125**, 531 (1986).
[11]Z. C. Ying and W. Ho, J. Chem. Phys. **91**, 5050 (1989).
[12]A. Szabó, M. Kiskinova, and J. T. Yates, J. Chem. Phys. **90**, 4604 (1989).
[13]P. M. Ferm, F. Budde, A. V. Hamza, S. Jakubith, D. Wiede, P. Andresen, and H. J. Freund, Surf. Sci. **218**, 467 (1989).
[14]Y. Yoshinobu, X. Guo, and J. T. Yates, Jr., J. Chem. Phys. **92**, 7700 (1990).
[15]A. R. Burns, E. B. Stechel, and D. R. Jennison, Phys. Rev. Lett. **58**, 250 (1987).
[16]A. R. Burns, D. R. Jennison, and E. B. Stechel, J. Vac. Sci. Technol. A **5**, 671 (1987).
[17]A. R. Burns, E. B. Stechel, and D. R. Jennsion, J. Vac. Sci. Technol. A **6**, 895 (1988).
[18]A. R. Burns, D. R. Jennison, and E. B. Stechel, J. Vac. Sci. Technol. A **8**, 2705 (1990).
[19]D. R. Jennison, E. B. Stechel, and A. R. Burns, in *Desorption Induced by Electronic Transitions, DIET III,* edited by R. H. Stulen and M. L. Knotek (Springer-Verlag, New York, 1988), pp. 67–72, 136–143, and 167–172.
[20]A. R. Burns, D. R. Jennison, and E. B. Stechel, Phys. Rev. B **40**, 9485 (1989).
[21]C. R. Brundle, P. S. Bagus, D. Menzel, and K. Hermann, Phys. Rev. B **24**, 7041 (1981).
[22]S. H. Lamson and R. P. Messsmer, Phys. Rev. B **25**, 7209 (1982).
[23]D. Heskett, E. W. Plummer, and R. P. Messmer, Surf. Sci. **139**, 558 (1984).
[24]J. L. Gland and E. B. Kollin, Surf. Sci. **151**, 260 (1985).
[25]M. Kiskinova, G. Pirug, and H. P. Bonzel, Surf. Sci. **140**, 1 (1984).
[26]G. Odorfer, E. W. Plummer, H.-J. Freund, H. Kuhlenbeck,

and M. Neumann, Surf. Sci. **198**, 331 (1988).
[27]J. L. Gland and B. A. Sexton, Surf. Sci. **94**, 355 (1980).
[28]D. H. Parker, M. E. Bartram, and B. E. Koel, Surf. Sci. **217**, 489 (1989).
[29]K. Mortensen, C. Klink, F. Jensen, F. Besenbacher, and I. Stensgaard, Surf. Sci. **220**, L701 (1989).
[30]Cut and polished by Metal Crystals + Oxides, LTD, Cambridge, England.
[31]J. L. Gland, B. A. Sexton, and G. B. Fischer, Surf. Sci. **95**, 587 (1980).
[32]Gerhard Herzberg, *Spectra of Diatomic Molecules,* 2nd ed. (Van Nostrand Reinhold, New York, 1950), pp. 264 and 558.
[33]D. C. Jacobs, R. J. Madix, and R. N. Zare, J. Chem. Phys. **85**, 5469 (1986).
[34]Lester T. Earls, Phys. Rev. **48**, 423 (1935).
[35]S. A. Buntin, L. J. Richter, D. S. King, and R. R. Cavanagh, J. Chem. Phys. **91**, 6429 (1989).
[36]K. P. Huber and G. Herzberg, *Molecular Spectra and Molecular Structure* (Van Nostrand Reinhold, New York, 1979), Vol. IV.
[37]M. P. Seah, Surf. Sci. **17**, 132 (1969).
[38]R. M. Lambert and C. M. Comrie, Surf. Sci. **38**, 197 (1973).
[39]J. P. Cowin, D. J. Auerbach, C. Becker, and L. Wharton, Surf. Sci. **78**, 545 (1978).
[40]F. P. Netzer and T. E. Madey, Surf. Sci. **110**, 251 (1981).
[41]G. Ertl and J. Küppers, *Low Energy Electrons and Surface Chemistry,* 2nd ed. (VCH Verlagsgesellschaft, Weinheim, 1985), p. 42.
[42]W. Ranke, Surf. Sci. **209**, 57 (1989).
[43]V. Dose, Surf. Sci. Rep. **5**, 337 (1985).
[44]A. R. Burns, D. R. Jennison, and E. B. Stechel, in *Desorption Induced by Electronic Transitions, DIET IV,* edited by G. Betz and P. Varga (Springer-Verlag, New York, 1990), pp. 41–45 and 182–186.
[45]J. C. Lin and R. Gomer, Surf. Sci. **218**, 406 (1989).
[46]R. Hoffmann, Rev. Mod. Phys. **60**, 601 (1988).
[47]G. Pacchioni and P. S. Bagus, J. Chem. Phys. **93**, 1209 (1990).
[48]P. Feulner, S. Auer, T. Müller, A. Puschmann, and D. Menzel, in *Desorption Induced by Electronic Transitions, DIET III* (Ref. 19), pp. 58–66.
[49]E. Umbach and Z. Hussain, Phys. Rev. Lett. **52**, 457 (1984).
[50]D. Menzel, P. Feulner, R. Treichler, E. Umbach, and W. Wurth, Phys. Scr. **T17**, 166 (1987).
[51]D. R. Jennison and D. Emin, Phys. Rev. Lett. **51**, 1390 (1983).
[52]A. R. Burns, T. M. Orlando, E. B. Stechel, and D. R. Jennison, J. Vac. Sci. Technol. A **9**, 1774 (1991); Phys. Rev. B (to be published).
[53]J. E. Smedley, G. C. Long, and M. H. Alexander, J. Chem. Phys. **87**, 3218 (1987).
[54]H. Lefebvre-Brion and R. W. Field, *Perturbations in the Spectra of Diatomic Molecules* (Academic, New York, 1986).
[55]M. Wohlecke and G. Borstel, in *Spin-Polarized Photoelectrons and Crystal Symmetry,* edited by F. Meier and B. P. Zakharchenya (Elsevier Science, New York, 1984), pp. 425–462, and references therein.
[56]A. Eyers *et al.*, Phys. Rev. Lett. **52**, 1559 (1984).
[57]J. Kirschner, *Polarized Electrons at Surfaces* (Springer-Verlag, New York, 1985), and references therein.
[58]O. K. Andersen, Phys. Rev. B **2**, 883 (1970).
[59]E. Hasselbrink, Chem. Phys. Lett. **170**, 329 (1990).
[60]E. Hasselbrink, S. Jakubith, S. Nettesheim, M. Wolk, A. Cassuto, and G. Ertl, J. Chem. Phys. **92**, 3154 (1990).
[61]C. W. Muhlhausen, L. R. Williams, and J. C. Tully, J. Chem. Phys. **83**, 2594 (1985); J. C. Tully and M. J. Cardillo, Science **223**, 445 (1984).